John von Neumann Institute for Computing

Zener Breakdown in Superlattices

Stephan Glutsch

published in

NIC Symposium 2001, Proceedings,
Horst Rollnik, Dietrich Wolf (Editors),
John von Neumann Institute for Computing, Jülich,
NIC Series, Vol. **9**, ISBN 3-00-009055-X, pp. 271-280, 2002.

http://www.fz-juelich.de/nic-series/volume9

Zener Breakdown in Superlattices

Stephan Glutsch

Institut für Festkörpertheorie und Theoretische Optik
Friedrich-Schiller-Universität Jena
Max-Wien-Platz 1, 07743 Jena, Germany
E-mail: stephan@ifto.physik.uni-jena.de

In this paper we provide numerical and experimental evidence for the Zener breakdown in the optical spectrum of superlattices. It is demonstrated that the assumption of Wannier-Stark ladders and the Kane approximation are not justified in the regime of the Zener breakdown. The numerical calculation of the absorption spectrum, including Coulomb interaction, is performed by solving an initial-value problem, where the Hamiltonian in real space is discretized by finite differences. The method is highly efficient and perfectly suitable for vector machines. Storage and computing time scale like $O(N)$, where N is the number of grid points.

1 Introduction

In 1960, Wannier[1] discovered that the energy spectrum of a Bloch electron in an electric field consists of equally spaced eigenvalues, but also argued that the eigenfunctions are not normalizable and should therefore not lead to stationary states. On the other hand, the most common approximations, the discrete model,[2] the tight-binding model,[3] and the one-band approximation,[4] lead to localized wave functions, and it was a common belief for a long time that the spectrum of a Bloch electron in an electric field would be discrete. Eventually the continuous nature of the spectrum was rigorously established by Avron *et al*.[5] Nevertheless, from the practical point of view, the notion of "Wannier-Stark resonances" is justified when the lifetime broadening is much smaller than the level spacing.[6]

In 1988, Wannier-Stark quantization was observed experimentally in photoluminescence, photocurrent, and photoluminescence excitation spectroscopy on superlattices[7,8] and Bloch oscillations were measured in time-resolved and spectrally resolved four-wave-mixing experiments.[9]

Traditionally, these experiments have been described in terms of Wannier-Stark ladders. It was shown that the Wannier-Stark ladder picture suffices to explain absorption measurements[7,8,10–12] as well as nonlinear optical experiments.[9,13] For high electric fields, Zener tunneling is expected to take place. Signatures of Zener tunneling have been reported in recent years.[14–16] These papers mainly focus on the coupling of a finite number of minibands, also known as resonant Zener tunneling.

In the original paper, the Zener effect describes an open system with tunneling between one band and the continuum of all other bands under the influence of an electric field F.[17,18] The tunneling rate γ for interminiband transitions is equal to

$$\gamma = \frac{e|F|a}{2\pi\hbar} \exp\left[-\frac{m_{\mathrm{e}} a(\Delta E)^2}{4\hbar^2 e|F|}\right], \tag{1}$$

where m_{e} is the effective electron mass, a is the superlattice period, and ΔE is the gap between first and second miniband. This result was derived for nearly free electrons, under

the assumption that the other gaps are significantly smaller than ΔE. The quantity $\hbar\gamma$ can be considered as the imaginary part of the eigenvalues, which leads to an exponential decrease of the wavefunction and to a broadening in the optical spectrum. This non-resonant Zener tunneling has been observed in the optical absorption of strongly coupled superlattices,[19] and has been explained mainly in term of interaction-free electrons and holes.[20]

A particularly difficult problem is the calculation of the optical absorption in low-dimensional semiconductors. The interband absorption is related to the eigenvalue problem of an electron-hole pair, subjected to Coulomb interaction, geometric confinement, and external fields,[21–23] which is in general a partial differential equation with up to six variables. The spectrum can be entirely discrete or possess a one- or many-parametric continuum. Only in very few cases with high symmetry, the problem can be solved analytically.

In the general case, the optical absorption has to be calculated numerically. This has been done by solving eigenvalue or boundary-value problems by exact or iterative methods.[24–26] So far, in the case that the continuous spectrum of the electron-hole Hamiltonian is effectively one-parametric, the reformulation as a scattering problem proved to be most efficient, leading to very accurate results.[10, 27–29]

However, in the case that the continuum is two- or more-parametric, like in superlattices, conventional methods are not applicable. A highly efficient method, based upon discretization of the operator in real space and solution of an initial-value problem, which was developed by the author,[30] is able to calculate optical spectra of the most complicated geometries, such as quantum wires, superlattices in electric and magnetic fields, or excitons on rough interfaces in many dimensions. Equation-of-motion methods are frequently used in quantum chemistry, solid-state physics, and material science.[31–33] In many cases, memory and computing time can be further reduced considerably by the introduction of absorbing boundary conditions, as demonstrated by Ahland *et al.*[34]

The paper is organized as follows. In Sec. 2, we consider the one-particle problem of an electron or hole in a superlattice with applied electric field. A brief introduction into methods of calculating the optical absorption of low-dimensional semiconductors is given in Sec. 3. In Sec. 4, we calculate the absorption of a superlattice for realistic parameters. The numerical results are compared with experimental spectra. Finally, a summary and conclusions are given in Sec. 5.

2 One-Particle Problem

We consider a particle with charge q and mass m in a one-dimensional periodic potential U with the period a, subjected to an electric field F. A periodic potential, which is typically realized in a superlattice, is shown in Fig. 1. The eigenvalues and eigenfunctions obey the following equation:

$$\Big[-\frac{\hbar^2}{2m} \frac{d^2}{dz^2} + U(z) - qFz \Big] \varphi_\lambda(z) = E_\lambda \varphi_\lambda(z) \,. \tag{2}$$

In case that $U(z) = 0$ and $F \neq 0$, the spectrum is entirely continuous and the eigenfunctions are given by the Airy function.[35] For $U(z) \neq 0$ and $F = 0$, the eigenvalues and eigenfunctions $\varepsilon_\lambda(k)$ and $\psi_{k\lambda}$ obey the Bloch theorem. There is no simple rule how the spectrum looks like in the general case $U \neq 0$ and $F \neq 0$, for example, whether the eigenvalues are discrete or continuous. We only know that, if E is an eigenvalue with

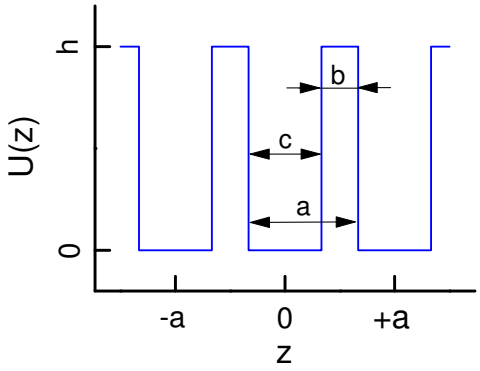

Figure 1. Sketch of the periodic potential U.

normalizable or non-normalizable eigenfunction $\varphi(z)$, then $E - qFam; m \in \mathbb{Z}$ is also an eigenvalue, and the corresponding eigenfunction is $\varphi(z - ma)$. This was already observed in the original paper by Wannier.[1]

In order to get a feeling about te structure of the solution, we construct a discrete model

$$\sum_{n'} \Big[A\,\delta_{nn'} - B\,(\delta_{n,n-1}+\delta_{n,n+1}) + f\,n\,\delta_{nn'} \Big]\, w_{n'} = E\,w_n\,. \tag{3}$$

The solution can be found analytically and for a non-zero field f it holds that[2]

$$E_m = A + fm\;; \quad m \in \mathbb{Z} \quad w_{m;n} = J_{m-n}(\frac{2B}{f})\;; \quad \sum_n w_{m;n}\,w_{m';n} = \delta_{mm'}\,. \tag{4}$$

The spectrum is entirely discrete and the eigenvectors are normalizable. The real constants A, B, and f can be identified with the parameters of the tight-binding model with next-neighbor interaction. Then, in principle, each below-barrier state of the single quantum well leads to a Wannier-Stark ladder. For above-barrier states, which are not localized, the procedure is not applicable, which suggests that those states give rise to a continuum for $F \neq 0$.

In the Kane approximation, the Hamiltonian is projected onto the individual subbands λ. Then the eigenvalues and eigenfunctions (Kane or Houston functions) are:[4]

$$\begin{aligned} E_{\lambda m} &= \frac{a}{2\pi} \int\limits_{-\pi/a}^{+\pi/a} dk \Big[\varepsilon_\lambda(k) - qFZ_{\lambda\lambda}(k) \Big] + meFa \\ \varphi_{\lambda m}(z) &= \Big(\frac{a}{2\pi}\Big)^{1/2} \int\limits_{-\pi/a}^{+\pi/a} dk\,\tilde{\varphi}_{\lambda m}(k)\,\psi_{k\lambda}(z)\,, \end{aligned} \tag{5}$$

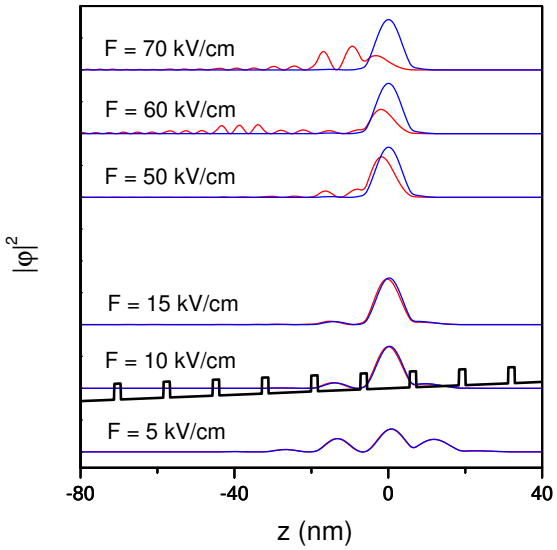

Figure 2. Probability density as function of the coordinate for different electric fields. Blue line: Kane approximation, red line: full numerical solution.

where

$$\tilde{\varphi}_{\lambda n}(k) = \exp\left\{ \frac{1}{-iqF} \int_0^k dk' \left[E_{\lambda m} - \varepsilon_\lambda(k') - eFZ_{\lambda\lambda}(k') \right] \right\}$$
$$Z_{\lambda\lambda}(k) = \frac{i}{a} \int_{-a/2}^{+a/2} dz\, u^*_{k\lambda}(z) \frac{\partial u_{k\lambda}(z)}{\partial k} . \tag{6}$$

The normalization of the Bloch functions is assumed to be $\delta_{\lambda\lambda'}\,\delta(k-k')$ modulo $2\pi/a$. This time, there is no difference between below- and above-barrier states: every miniband λ leads to a Wannier-Stark ladder $E_{\lambda m}$.

With increasing field, the localization of the Kane functions increases. It can be shown[36] that the extension of the Kane function is of the form $\sqrt{a^2 + b^2/F^2}$. For $|F| \to \infty$, the Kane function goes over in the Wannier function. This picture seems not to be realistic for large fields or weak confinement: if the modulation of the periodic potential is negligible, compared to qFa, then the eigenfunctions should qualitatively behave like the Airy function and the spectrum should be continuous. It can indeed be shown that the spectrum is entirely continuous for arbitrary F, but the proof is intricate.[5] On the other hand, the spectrum can show resonances with a very small width, which behave like discrete eigenvalues. Practically, we expect expect three regions: the region of small fields, when the Kane approximation is justified, a transition region for medium fields, and a region of large fields, when the Kane approximation breaks down and the spectrum becomes a structureless continuum.

In order to study the accuracy of the Kane approximation, we make a comparison be-

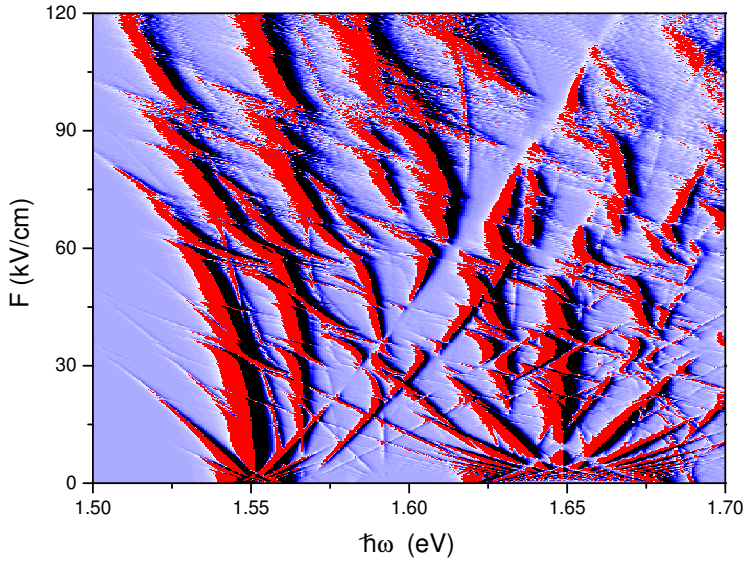

Figure 3. Optical density of states as function of the photon energy and the electric field.

tween the Kane approximation (5) and the result of a numerical solution of Eq. (2), based upon finite differences. We use the parameters of the conduction electron in a 111/17 Å $GaAs/Ga_{0.7}Al_{0.3}As$ superlattice: $q_e = -e$, $m_e = 0.067\,m_0$, $a = 12.8\,\mathrm{nm}$, $b = 1.7\,\mathrm{nm}$, $c = 11.1\,\mathrm{nm}$, and $h_e = 237\,\mathrm{meV}$. The result is shown in Fig. 2. The probability density $|\varphi|^2$ is plotted versus z for various fields $F = 5 \ldots 70\,\mathrm{kV/cm}$. For low electric fields, $F \leq 15\,\mathrm{kV/cm}$, the Kane function (blue) and the exact solution (red) are virtually undistinguishable. For high fields, $F \geq 50\,\mathrm{kV/cm}$, the Kane function approaches the Wannier function and becomes independent of the electric field. In contrast, the exact solution shows a strong tunneling through the barrier, leading to delocalization. The tail for $z \to -\infty$ qualitatively behaves like the solution for $U = 0$.

The delocalization of the eigenfunctions has consequences for the optical absorption. For localized eigenfunctions, we expect sharp resonances, while for delocalized eigenfunctions absorption should become entirely continuous. In the one-particle picture, the optical absorption can be characterized by the joint density of states

$$D(\omega) = \frac{1}{L} \sum_{\lambda\lambda'} \left| \int_{-\infty}^{+\infty} dz\, \varphi_{e\lambda}(z)\, \varphi_{h\lambda'}(z) \right|^2 \pi\, \delta\Big[\, \hbar\omega - (E_{e\lambda} + E_{h\lambda'} + E_g) \Big]. \quad (7)$$

Here, $\varphi_{e\lambda}$ and $\varphi_{h\lambda}$ are the eigenfunctions of electron and hole with energies $E_{e\lambda}$ and $E_{h\lambda}$. The eigenvalue problem for the hole follows from Eq. (2) by replacing m_e by m_h and $-e$ by $+e$. The normalization length is considered in the limit $L \to \infty$. The hole parameters for the GaAs/(Ga,Al)As superlattice under consideration are $q_h = +e$, $m_h = 0.45\,m_0$ and $h_h = 63.2\,\mathrm{meV}$. The band gap of GaAs is $E_g = 1.52\,\mathrm{eV}$.

The optical density D as function of the photon energy $\hbar\omega$ and the electric field is shown in Fig. 3. For low values of the electric fields, we observe two Wannier-Stark

ladders, associated with the (1,1) and (2,2) transitions. The positions of the resonances scales linear with field and the distance between subsequent lines of the Wannier-Stark ladders is $e\,F\,a$. With increasing field, the resonances shift to lower energies. Furthermore, we observe strong interactions between different Wannier-Stark ladders. For large fields, the Wannier-Stark ladders are destroyed. For the (2,2) ladder, this is the case for $F \geq 50\,\mathrm{kV/cm}$. The (1,1) ladder disappears at about $F = 60\,\mathrm{kV/cm}$. The remaining resonances cannot be directly attributed to a Wannier-Stark ladder and are strongly broadened. The situation is similar to a bulk semiconductor in an electric field, where the spectrum shows Franz-Keldysh oscillations.

3 Numerical Method

The calculation of absorption spectra in low-dimensional semiconductors is very complicated, especially in cases where the continuum is more than one-parametric. This problem was the subject of numerous papers in the last decade. Here, we give a brief overview over different methods of calculating the optical absorption.

The absorption coefficient $\alpha(\omega)$ is proportional to the imaginary part of the optical susceptibility $\chi(\omega)$. Generally, the optical susceptibility of a low-dimensional semiconductor (in dimensionless units) is given by[21–23]

$$\begin{aligned} \chi(\omega) &= \sum_{\Lambda} \frac{|\langle\, \mu \,|\, \Phi_\Lambda \,\rangle|^2}{E_\Lambda - (\omega + i\epsilon)} \\ \hat{H}\,|\,\Phi_\Lambda\,\rangle &= E_\Lambda\,|\,\Phi_\Lambda\,\rangle\,; \quad \langle\,\Phi_\Lambda\,|\,\Phi_{\Lambda'}\,\rangle = \delta_{\Lambda\Lambda'}\,, \end{aligned} \tag{8}$$

where $\hat{H}$ is the electron-hole-pair Hamiltonian, which is a differential operator in up to six variables, $|\,\mu\,\rangle$ is the dipole matrix element, and $\epsilon = +0$ is a positive infinitesimal. In reality, ϵ is finite, and is identical to the homogeneous line broadening. After discretization of $\hat{H}$, the numerical effort for the diagonalization is in the order of N^3, where N is the dimension of the matrix H. The dimension N, which can be handled, is in the order of a few thousands. Iterative methods, based upon the Lanczos algorithm are able to calculate the absorption spectrum in $O(N^2)$ operations.[24]

The representation (8) is equivalent to the following boundary-value problem:[27]

$$\chi(\omega) = \langle\,\mu\,|\,\left[\,\hat{H} - (\omega + i\epsilon)\,\right]^{-1}\,|\,\mu\,\rangle\,. \tag{9}$$

This time, a set of equations has to be solved for each ω. The numerical effort is $O(N^3)$, if the matrix H is fully occupied, but can be significantly larger if H is tridiagonal or banded. Tridiagonal or banded matrices result from the discretization of one-dimensional problems or multi-dimensional problems, when the domain is very anisotropic, like quantum wells or quantum wires. For multi-parametric continua, the solution as a boundary-value problem is not practicable.

Both the eigenvalue and the boundary-value problem can be reformulated as a scattering problem.[10,27,29] This method is highly accurate and efficient, but is limited to problems with one continuum direction.

By Fourier transform, Eq. (9) goes over into[30]

$$\chi(\omega) = i \int_0^\infty dt\, e^{i(\omega+i\epsilon)t} \langle\, \mu \,|\, \Psi \,\rangle \;; \quad i\frac{d}{dt} \,|\, \Psi(t) \,\rangle = \hat{H} \,|\, \Psi(t) \,\rangle \;; \quad |\, \Psi(0) \,\rangle = |\, \mu \,\rangle \,, \tag{10}$$

which requires the solution of a Schrödinger initial-value problem. If $\hat{H}$ is discretized in real space, using finite differences, the matrix H is (irregularly) sparse and the calculation of the spectrum takes only $O(N)$ operations, independent of the dimensionality and the domain. Furthermore, for regular meshes, the algorithm is ideally suitable for vector machines. The method allows to calculate the optical response for the most difficult geometries.

A significant reduction of the storage and the computational effort can be achieved by means of absorbing boundary conditions. Ahland *et al.* used a complex coordinate transform, leading to decrease of the wavepacket in the absorption layer.[34] An alternative formulation, used by the author, is the introduction of a complex effective mass inside the absorption layer.[37]

4 Optical Absorption

The Hamiltonian of the electron-hole pair in a superlattice, in the presence of an electric field in growth direction is

$$\begin{aligned} \hat{H} = &-\frac{\hbar^2}{2m_\rho}\Delta_\rho - \frac{\hbar^2}{2m_\mathrm{e}}\frac{\partial^2}{\partial z_\mathrm{e}^2} - \frac{\hbar^2}{2m_{\mathrm{h}z}}\frac{\partial^2}{\partial z_\mathrm{h}^2} + U_\mathrm{e}(z_\mathrm{e}) + U_\mathrm{h}(z_\mathrm{h}) \\ &+ F(z_\mathrm{e}{-}z_\mathrm{h}) - \frac{1}{\sqrt{\rho^2 + (z_\mathrm{e}{-}z_\mathrm{h})^2}} \,. \end{aligned} \tag{11}$$

This time, we take into account the unisotropy of the hole mass. The parallel and perpendicular hole masses are $m_{\mathrm{h}z} = 0.377\, m_0$ and $m_{\mathrm{h}\rho} = 0.491\, m_0$. The parallel reduced mass is $m_\rho = m_\mathrm{e} m_{\mathrm{h}\rho}/(m_\mathrm{e}{+}m_{\mathrm{h}\rho})$. The dipole moment is $\mu(\rho) \propto \delta(\rho)\, \delta(z_\mathrm{e} - z_\mathrm{h})/(2\pi\rho)$ and the volume element, which enters the definition of the scalar product (10), is $2\pi\rho\, d\rho\, dz_\mathrm{e}\, dz_\mathrm{h}$.

For the numerical solution, we introduced center and relative coordinates $Z = z_\mathrm{e} \in [\,0\,,\, a\,]$ and $z = z_\mathrm{e} - z_\mathrm{h} \in (\,-\infty\,,\, +\infty)$. This choice ensures that the mesh points for z_e and z_h are identical. The Bloch theorem can be applied for the variable Z and only those eigenfunctions contribute to the optical absorption, which are periodic in Z. The eigenvalue problem was rewritten as an initial-value problem (10) and absorbing boundary conditions were used for the radial direction. The total number of grid points was in the order of 10 million.

We calculated the optical absorption for a 76/39 Å $\mathrm{GaAs}/\mathrm{Ga_{0.92}Al_{0.08}As}$ superlattice. Due to the small Al content of 8 %, the barriers are very shallow, $h_\mathrm{e} = 63.2\,\mathrm{meV}$ and $h_\mathrm{h} = 36.8\,\mathrm{meV}$, which leads to an increased tunneling probability. We compare the numerically exact solution with the approximate result, when the two-particle Hamiltonian is projected onto the electron and hole Kane function.

The result is shown in Fig. 4 a. The numerical exact result (red curve) is compared with the Kane approximation. For zero electric field, we observe an exciton peak and

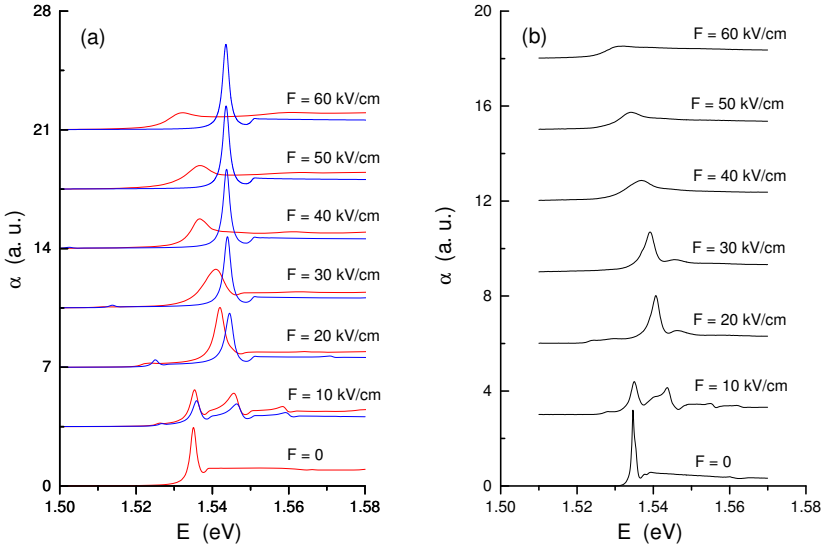

Figure 4. Absorption of the superlattice vs. photon energy for different values of the electric field. a) Full numerical solution (red) and result of the Kane approximation (blue). b) Experimental spectrum.

a flat continuum. For small fields, $F \leq 10\,\mathrm{kV/cm}$, we see one Wannier-Stark ladder, associated with the (1,1) transition. The lines are inhomogeneously broadened due to Fano interference. There is no qualitative difference between the exact and the approximate solution, although the influence of non-resonant subbands, neglected in the approximate solution, leads to an overall increase of the absorption. Starting at $F \geq 20\,\mathrm{kV/cm}$, exact and approximate solution behave differently. For the approximate solution, the absorption peak narrows and the oscillator strength increases with field. In contrast, in the exact solution, we observe a line broadening and a shift of the maximum to lower energies, which is a result of Zener tunneling. For very large fields, $F \geq 50\,\mathrm{kV/cm}$, the absorption becomes a flat continuum.

Figure 4 b shows experimental results, obtained by Rosam and co-workers.[37] The experimental spectrum is very similar to the result of the full numerical solution. This is true for the Wannier-Stark ladder, the Fano interference, the line shift, and the broadening for large electric fields. On the other hand, the theoretical spectrum, based upon the Kane approximation, is not able to explain the experimental results for large electric fields.

Finally, we compare the measured linewidth with the prediction of the Zener model (1). For this reason, we compare the linewidth (HWHM) with the function

$$\hbar\gamma = \frac{e}{2\pi}\, A\, F\, \exp(-\frac{B}{F}) + C \tag{12}$$

where A, B, and C are fitting parameters. The result is shown in Fig. 5. The function (12) is shown by a solid line, while the blue circles represent the experimental values. For the fitting parameters, we obtain $A = 6.09\,\mathrm{nm}$, $B = 21.8\,\mathrm{kV/cm}$, and $C = 0.632\,\mathrm{meV}$. The values of A and B are in the order of values expected from Eq. (1). The constant C is equal to the intrinsic broadening at $F = 0$, which is not considered in the Zener model.

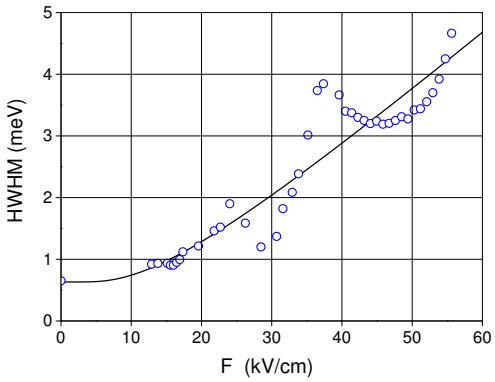

Figure 5. Linewidth vs. electric field. Blue circles: experimental values. Solid line: fit to Eq. (1) with $A = 6.09\,\mathrm{nm}$, $B = 21.8\,\mathrm{kV/cm}$, and $C = 0.632\,\mathrm{meV}$

The experimental linewidth shows strong oscillations, which result from anticrossing with other Wannier-Stark ladders (cf. Fig. 1).

5 Summary and Conclusions

In this paper we have demonstrated that Zener breakdown is realistic in semiconductor superlattices. The numerical calculation of the spectrum was performed by means of a highly efficient real-space-real-time method. The experimental results are in good agreement with the predictions of the theory. Meanwhile, the Zener breakdown has also been detected in a superlattice with perpendicular electric and magnetic fields. In this geometry, Fano interference is suppressed by the Landau quantization and a transition is observed between entirely discrete and continuum states.[38]

The calculations were performed on a Cray J 90 or T 90. Depending on the problem, the computing time was between 3 days and 3 weeks.

Acknowledgments

The author is indebted to K. Leo and B. Rosam for contributing the experimental results. Computing time from the John von Neumann Institute for Computing, Research Center Jülich, is gratefully acknowledged.

References

1. G. H. Wannier, Phys. Rev. **117**, 432 (1960).
2. K. Hacker and G. Obermair, Z. Physik **234**, 1 (1970).
3. J. Bleuse, G. Bastard, and P. Voisin, Phys. Rev. Lett. **60**, 220 (1988).
4. E. O. Kane, J. Phys. Chem. Solids **12**, 181 (1959).
5. J. E. Avron, J. Zak, A. Grossmann, and L. Gunther, J. Math. Phys. **18**, 918 (1977).

6. A. Nenciu and G. Nenciu, J. Phys. A **15**, 3313 (1982).
7. E. E. Mendez, A. Agulló-Rueda, and J. M. Hong, Phys. Rev. Lett. **60**, 2426 (1988).
8. P. Voisin, J. Bleuse, C. Bouche, S. Gaillard, C. Alibert, and A. Regrency, Phys. Rev. Lett. **61**, 1639 (1988).
9. K. Leo, P. Haring Bolivar, F. Brüggemann, R. Schwedler, and K. Köhler, Solid State Comm. **84**, 943 (1992).
10. D. M. Whittaker, Europhys. Lett. **31**, 55 (1995).
11. C. P. Holfeld, F. Löser, M. Sudzius, K. Leo, D. M. Whittaker, and K. Köhler, Phys. Rev. Lett. **81**, 874 (1998).
12. A. Thränhardt, H.-J. Kolbe, J. Hader, T. Meier, G. Weiser, and S. W. Koch, Appl. Phys. Lett. **73**, 2612 (1998).
13. M. M. Dignam, J. E. Sipe, and J. Shah, Phys. Rev. B **49**, 10 502 (1994).
14. H. Schneider, H. T. Grahn, K. v. Klitzing, and K. Ploog, Phys. Rev. Lett. **65**, 2720 (1990).
15. A. Sibille, J. F. Palmier, and F. Laruelle, Phys. Rev. Lett. **80**, 4506 (1998).
16. M. Helm, W. Hilber, R. De Meester, F. M. Peeters, and A. Wacker, Phys. Rev. Lett. **82**, 3120 (1999).
17. C. Zener, Proc. Roy. Soc. **145**, 523 (1934).
18. Qian Niu and M. G. Raizen, Phys. Rev. Lett. **80**, 3491 (1998).
19. B. Rosam, F. Löser, V. G. Lyssenko, K. Leo, S. Glutsch, F. Bechstedt, and K. Köhler, Physica B **272**, 180 (1999).
20. S. Glutsch and F. Bechstedt, Phys. Rev. B **60**, 16 584 (1999).
21. R. J. Elliott, Phys. Rev. **108**, 1384 (1957).
22. *Polarons and Excitons,* Ed. by C. G. Kuper and G. D. Whitfield (Oliver and Boyd, Edinburgh and London, 1963).
23. J. O. Dimmock, in *Semiconductors and Semimetals,* ed. by R. K. Willardson and A. C. Beer, Vol. 3 (Academic Press, New York, 1967).
24. Chu and Y.-C. Chang, Phys. Rev. B **40**, 5497 (1989).
25. C. Stafford, S, Schmitt-Rink, and W. Schäfer, Phys. Rev. B **41**, 10 000 (1990).
26. R. Winkler, Phys. Rev. B **51**, 14 395 (1995).
27. R. Zimmermann, phys. stat. sol. (b) **135**, 681 (1986).
28. M. Graf, P. Vogl, and A. B. Dzyubenko, Phys. Rev. B **54**, 17 003 (1996).
29. K. Hino, Phys. Rev. B **62**, 10 626 (2000).
30. S. Glutsch, D. S. Chemla, and F. Bechstedt, Phys. Rev. B **54**, 11 592 (1996).
31. R. Kosloff, J. Phys. Chem. **92**, 2087 (1988).
32. N. A. Hill and K. B. Whaley, J. Chem. Phys. **99**, 3707 (1993).
33. D. Hobbs, D. Weaire, S. McMurry, and O. Zuchuat, J. Phys.: Condens. Matter **8**, 4691 (1996).
34. A. Ahland, D. Schulz, and E. Voges, Phys. Rev. B **60**, 5109 (1999).
35. L. D. Landau and E. M. Lifshitz, *Course of Theoretical Physics,* Vol. 3, 3rd. ed. (Pergamon, New York, 1987).
36. S. Glutsch, J. Phys.: Condens. Matter **11**, 5533 (1999).
37. S. Glutsch, F. Bechstedt, B. Rosam, and K. Leo, Phys. Rev. B **63**, 085307 (2001).
38. D. Meinhold, K. Leo, N. A. Fromer, D. S. Chemla, S, Glutsch, F. Bechstedt, and K. Köhler, submitted to Phys. Rev. B.